Liposome-induced DNA compaction and reentrant condensation investigated by dielectric relaxation spectroscopy and dynamic light scattering techniques

S. Zuzzi,[1,2] C. Cametti,[2,*] G. Onori,[2] and S. Sennato[1]
[1]*Dipartimento di Fisica and INFM-CRS SOFT, Università di Roma "La Sapienza," Piazzale A. Moro 2, I-00185 Rome, Italy*
[2]*Dipartimento di Fisica, INFM-CRS SOFT, Unità di Perugia, Università di Perugia and CEMIN (Centro Eccellenza Materiali Innovativi Nanostrutturati), Via A. Pascoli, I-06123, Perugia, Italy*
(Received 30 April 2007; published 30 July 2007)

Interaction of DNA with oppositely charged objects, such as multivalent ions, cationic surfactants, cationic liposomes, basic proteins, and alcohols, up to nano- or mesoscopic particles, gives rise to a very interesting and fascinating phenomenology, where the shape, size, and stability of the resulting aggregates depend on a delicate balance between different driving forces, mainly of electrostatic origin. We have studied the cationic liposome-DNA complexes during the whole complexation process, below, close to, and above the isoelectric condition, where the number of cationic lipids equals the number of phosphate groups on the DNA chain. We took advantage of the combined use of dynamic light scattering, laser Doppler electrophoretic mobility, and radio-wave dielectric relaxation measurements in order to characterize both the structural parameters (hydrodynamic radius) and the electrical parameters (charge and counterion concentration) of the resulting structures. These structures are fundamentally of two types, clusters of liposomes stuck together by DNA chains (cluster phase in low-density colloidal suspension) and coexisting DNA coils and DNA globules, according to the procedure through which interactions occur (liposomes in excess DNA solution or DNA in excess liposome suspension).

DOI: 10.1103/PhysRevE.76.011925 PACS number(s): 87.15.Kg, 82.70.Dd, 61.25.Hq, 82.70.Uv

I. INTRODUCTION

Interactions of DNA with oppositely charged objects (compaction agents) give rise to a very complex phenomenology, depending on their physicochemical properties and on their chemical nature. Recently, Zinchenko and Chen [1] have summarized this phenomenology and have classified these agents into four different kinds, according to their dimensionality. In particular, they refer to zero-dimensional (multivalent cations), one-dimensional (polycations with charges distributed along the polymer chain), two-dimensional (cationic surfaces), and three-dimensional (nano- or mesoscopic three-dimensional structures) agents. Each of these different compaction agents induces different intricate topological rearrangements, including DNA condensation, DNA compaction, liposome aggregation, and liposome fusion.

The processes of interaction and binding of cationic lipidic bilayers are of great importance in a variety of biotechnological applications [2], and have been extensively investigated in view of the potential use of these systems as vehicles for gene delivery and gene transfection [3].

Although DNA compaction by cationic surfactants has been extensively studied in recent years [4–7], DNA interactions with differently structured mesoscopic particles have been studied to a much lesser extent [8].

As pointed out by Zinchenco and Chen [1], according to the size of the mesoscopic particles and the length of the DNA chain, DNA compaction can occur either when DNA is freely adsorbed on the surface of the object (preferentially for low-molecular-weight DNA and large surfaces) or when DNA collects relatively small-size particles along its chain (preferentially for high-molecular-weight DNA). Both these two modalities produce different single DNA chain–mesoscopic particle structures which further evolve toward differently organized aggregates.

Here, we will focus on interactions of DNA chains with double-chain cationic lipids (dideoyl trimethylammonium propane [DOTAP]) organized in vesicle particles (liposomes), which represent the higher level in the hierarchy of DNA compacting agents (three-dimensional agents). Interactions will occur in two different environments (DNA-rich solution and liposome-rich solution, respectively) and will produce two completely different structural aggregates.

The first of them (addition of lipid to DNA solution, DNA-rich environment) resembles the DNA solution, where the DNA chains change in a discrete manner between elongated coils and compacted globules. The transition between random coils and compact globules has been previously observed on the basis of fluorescence microscopy measurements by Mel'nikov *et al.* [4], who carried out a quantitative analysis of the change of various physical parameters of the DNA chain (long axis length, translational diffusion coefficient, and radius of gyration) upon addition of a single-chain cationic surfactant, cetyl trimethyl ammonium bromide (CTAB). This DNA compaction differs from the usual DNA condensation induced by multivalent counterions, where the increase of the ionic strength provokes a "first-order" phase transition [9,10] between an extended coil and a more compacted state.

The second one (addition of DNA to liposome suspension, lipid-rich environment) leads to the formation of large, nearly neutral, aggregates that constitute a new colloidal cluster phase with unusual and not yet completely under-

*Corresponding author. FAX: +39 064463158.
cesare.cametti@romal.infn.it

stood properties. This class of colloids is particularly intriguing [11,12]; they are systems characterized by the simultaneous presence of a short-range attraction and a screened electrostatic repulsion, whose shape and size are sensitively dependent on the balance between attraction and repulsion [13–15].

By means of a combined use of different experimental techniques (dynamic light scattering, laser Doppler electrophoretic mobility, and radio-wave dielectric relaxation measurements), we present a unifying picture of the conformational changes occurring in the DNA-DOTAP liposome system, by investigating a large interval in the DNA and DOTAP concentrations. We induced the DNA-DOTAP interactions and the consequent aggregate formation in two different ways, depending upon the modalities of addition of lipid to DNA or of DNA to lipid, which define the basic environmental conditions in which interactions occur (DNA-excess or lipid-excess conditions). Although two basically different structures are formed, we show that this complex phenomenology can be described within a unique frame, governed by the lipid-to-DNA charge ratio.

II. EXPERIMENT

A. Materials and sample preparation

Dioleoyl trimethyl ammonium propane (DOTAP) was purchased from Avanti Polar Lipids (Alabaster, Alabama) and was used without further purification. Double-stranded DNA sodium salt, purchased from Sigma Chemical Co., was fragmented by pulse-power mode sonication. The size distribution of the DNA molecules ranged from 500 to 1000 nucleotide pairs, as determined by agarose gel electrophoresis. Unilamellar liposomes were prepared by the standard lipid film hydration method. The lipid was dissolved in chloroform-methanol (1:1 vol/vol) at a concentration of 10 mg/ml. After solvent evaporation, dried lipid films were hydrated with deionized water (electrical conductivity less than $10^{-6}\ \Omega^{-1}\ \mathrm{cm}^{-1}$ at room temperature). In order to form unilamellar vesicles, the lipid solution was sonicated at a temperature of 25 °C for 1 h in pulsed-power mode until the solution appeared optically transparent in white light. The solution was later filtered through Millipore polycarbonate filters 0.45 μm in size. The liposome size and size distribution obtained from dynamic light scattering measurements give an average diameter of about 80 nm, with a moderate polydispersity of about 0.2, as expected for a rather homogeneous particle suspension.

The DNA-DOTAP liposome interaction was promoted in two different ways, the former by adding varying amounts (from 0 to 2.5 mg/ml) of DOTAP liposome suspension to a DNA solution at the fixed concentration of 0.75 mg/ml (interactions in DNA excess), and the latter by adding varying amounts of DNA solution (from 0 to 2 mg/ml) to a liposome suspension at a fixed concentration of 1.5 mg/ml (interaction in DOTAP excess). Although, in the two above-stated situations, we span a concentration range from below to above the isoelectric condition (at which the negative charges and the positive charges are stoichiometrically equal), the two emerging phenomenologies observed are rather different, with the presence of two basically different structures. In the former case, we observe structures with an overall negative charge (resembling the charge of the DNA chain), while, in the latter, we observe structures with an overall positive charge (resembling the charge of the liposomial vesicles). Moreover, in DNA-excess condition, lipids favor DNA compaction, inducing the collapse of the DNA molecules from an extended coil conformation to a compacted globular state. In the lipid-excess condition, on the contrary, the DNA chains act as an electrostatic glue for charged liposomes, favoring the formation of liposome aggregates that form a new cluster phase in low-density colloidal systems. Even more interestingly, we observe a continuous transition from one kind of structure to the other on varying the lipid-to-DNA charge ratio, opening the possibility of a unified description of the DNA-lipid complexes governed by electrostatic interactions.

B. Dynamic light scattering measurements

Dynamic light scattering measurements were performed using a Brookhaven digital BI-9000AT autocorrelator with a 10 mW He-Ne laser ($\lambda = 632.8$ nm). All measurements were taken at a scattering angle θ of 90°, at a fixed temperature of 25.0 ± 0.2 °C.

In the self-beating mode, the measured time-dependent photoelectron count autocorrelation function $G^{(2)}(q,\tau)$ has the form

$$G^{(2)}(q,\tau) = \int_0^\infty I(q,t)I(q,t+\tau)dt = A[1 + B|g^{(1)}(q,\tau)|^2], \tag{1}$$

where τ is the time delay, $g^{(1)}(q,\tau)$ is the first-order scattered electric field correlation function, $A = N_s\langle N\rangle$ is the baseline, with N_s the total number of samples and $\langle N\rangle$ the mean count per sample, B is a spatial coherence factor depending on the experimental setup, and q is the scattering wave vector, given by $q = (4\pi n/\lambda)\sin(\theta/2)$ with n and θ being the refractive index of the scattering medium and the scattering angle, respectively. For a dispersion of polydisperse particles, $g^{(1)} \times (q,\tau)$ takes the form

$$g^{(1)}(q,\tau) = \sum_i A_i e^{-D_i q^2 \tau}, \tag{2}$$

where A_i represent the scattering light amplitude of the particle i with diffusion coefficient D_i. Regularization methods such as CONTIN [16] and non-negatively constrained least squares [17] (NNLS) procedures were employed in analyzing the experimental data to solve Eq. (2) through eigenvalue decomposition, combined with a smoothing technique, in order to obtain the diffusion coefficients D_i. The size distribution function can be resolved in terms of the average hydrodynamic radius R_{Hi} by means of the Stokes-Einstein relationship $R_{Hi} = k_B T/6\pi\eta D_i$, where $k_B T$ is the thermal energy and η the viscosity of the aqueous phase.

C. Electrophoretic measurements

The measurements were carried out by means of the laser Doppler electrophoretic technique, using a Malvern Zeta-Sizer Nano apparatus equipped with a 5 mW He-Ne laser ($\lambda=632.8$ nm). The mobility u was converted into a ζ potential using the Smoluchowski relation $\zeta=u\eta/\epsilon$, where η and ϵ are the viscosity and the permittivity of the solution, respectively. All ζ-potential measurements were performed in pure water.

D. Radio-wave dielectric relaxation measurements

The permittivity $\epsilon'(\omega)$ and the electrical conductivity $\sigma(\omega)$ of DNA-liposome suspensions during the aggregation process have been measured in the frequency range from 100 Hz to 2 GHz, by means of two impedance analyzers (Hewlett-Packard models 4294A and 4291A), covering the frequency ranges 40 Hz–110 MHz and 1 MHz–2 GHz, respectively. Experiments were carried out at the temperature of 25.0 ± 0.2 °C. Details of the conversion from the measured electrical impedance of the measuring cell filled with the sample to be investigated and its dielectric properties [permittivity $\epsilon'(\omega)$ and electrical conductivity $\sigma(\omega)$] have been given elsewhere [18–20]. The dielectric spectra extend over a large frequency range, showing different dispersion regions, associated with the different conductive mechanisms occurring in the system, at a molecular level. In the intermediate frequency range, from about 10 to about 500 MHz, the dispersion associated with the dispersed mesoscopic objects predominates. This dispersion depends essentially on the counterion fluctuation along some typical particle lengths. Here, we will consider only this intermediate dispersion (once corrected for the electrode polarization effect), closely connected with the counterion atmosphere polarization induced by the applied electric field, and we will postpone to a later presentation the whole analysis of the dielectric behavior of the DNA-liposome aggregate suspension.

III. RESULTS

We are going to present and discuss separately the effects on the resulting aggregates obtained in the two different procedures we employed, addition of lipid to DNA and addition of DNA to lipid, respectively.

A. DOTAP liposome addition to a DNA solution

When cationic vesicles like, for example, DOTAP liposomes are added to the DNA solution above to a certain concentration, a coexistence region of some compacted DNA molecules (DNA globules) with DNA coils is evidenced. In this experimental procedure, the concentration of DNA was maintained constant at the value of $C=0.75$ mg/ml (about 2.3 mM/l, in terms of phosphate groups), and the content of liposomes was varied from $C_L=0.005$ to 2.5 mg/ml (corresponding to a vesicle concentration from 1.1×10^{11} to 5.7×10^{13} liposomes/ml).

In order to offer a first qualitative look at the system, we have to mention that, in these experimental conditions, the number of liposomes per DNA chain varies approximately from 0.001, at lower DOTAP concentration, to 0.5, at the higher DOTAP concentration investigated. However, the number of single DOTAP molecules per DNA chain is notably higher, considering that each liposome, 80 nm in diameter, contains approximately 3×10^4 monomers.

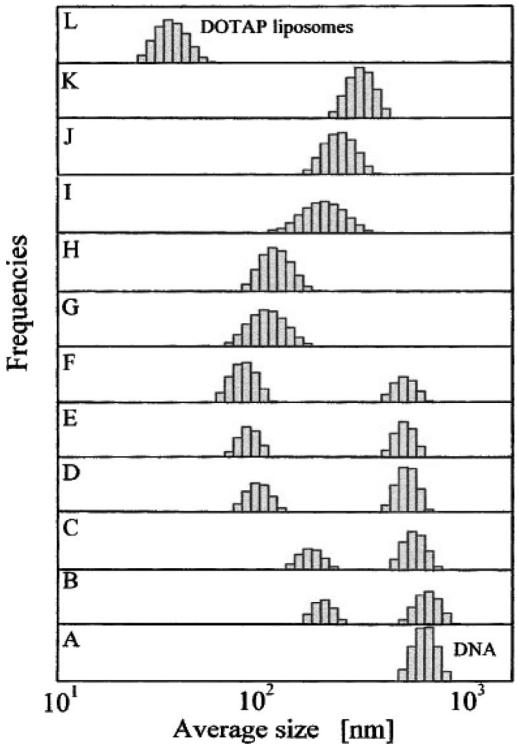

FIG. 1. Distribution of the hydrodynamic diameter of complexes formed between 0.75 mg/ml (2.3 mmol/l) DNA and DOTAP liposomes obtained from the intensity-weighted NNLS algorithm analysis at the temperature of 25 °C, at different DOTAP liposome content: (A) DNA solution, 0.75 mg/ml; (B) 0.005 mg/ml; (C) 0.0125 mg/ml; (D) 0.020 mg/ml; (E) 0.035 mg/ml; (F) 0.050 mg/ml; (G) 0.125 mg/ml; (H) 0.20 mg/ml; (I) 0.5 mg/ml; (J) 1.25 mg/ml; (K) 2.0 mg/ml; (L) DOTAP liposome suspension.

Typical results of the dynamic light scattering measurements are summarized in Fig. 1, where we show the deconvolution of the scattered light intensity correlation function $C(\tau)=\sqrt{G^{(2)}(q,\tau)-1}$ by means the algorithm NNLS [17] (the algorithm CONTIN [16] gives a substantially equivalent scenario). Starting from the bottom of the histograms shown in Fig. 2, for the DNA solution, the intensity-weighted correlation function presents only one peak, corresponding to the translational mode of the whole chain, giving a hydrodynamic radius of about 900 nm. The presentation of the size distribution on a log-probability graph results in an approximately symmetrical curve, as often happens when the size range is relatively large. For relatively long DNA strands, like those investigated in this study, the only contribution arises from the translational diffusion; as a consequence, the correlation function results in a unimodal distribution [21]. Moreover, at the DNA concentration employed (of the order of 2.3 mM/l in phosphate groups), no interactions between neighboring chains are expected.

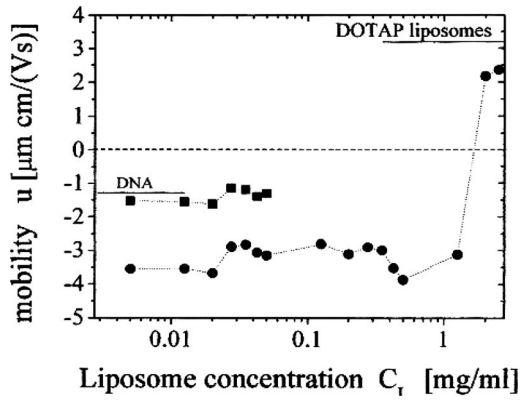

FIG. 2. Electrophoretic mobility of DNA solution with added DOTAP liposomes at different concentrations. At low to moderate liposome concentration, up to $C_L=0.06$ mg/ml, the spectrum shows two distinct peaks, corresponding to the unperturbed DNA chains and compacted DNA globules. The electrophoretic mobilities of DNA in the coil state (unperturbed) and of the single DOTAP liposomes are marked by horizontal straight lines. Below the isoelectric condition, in this case, close to 1 mg/ml, both the aggregates have an overall negative charge and a negative electrophoretic mobility. Above the isoelectric condition, charge inversion has occurred, the charge has became positive, and, correspondingly, the electrophoretic mobility inverts in sign (the dotted lines are to guide the eye only).

When the cationic vesicles are added to the DNA solution, the correlation function presents a bimodal distribution, the second peak of which corresponds to the more compacted structures with an average hydrodynamic diameter that progressively decreases, with the increase of the DOTAP liposome concentration, to values of the order of 100 nm. Moreover, with the increase of the liposome vesicle concentration, this second peak increases in amplitude, while the peak associated with the DNA translational mode decreases, until it disappears at a vesicle concentration of about 0.06–0.07 mg/ml. From this point on, only compacted globules are present. This finding supports evidence, among others [22], of the existence of two populations, one of unperturbed DNA coils coexisting with one of more compacted DNA globules.

This scenario is partially analogous to what happens when cationic surfactants such as, for example, tetradecyl ethyl ammonium bromide, cetyl trimethyl ammonium bromide or dedecyl trimethyl ammonium bromide, are added to the DNA solution at a concentration well below their critical micellar concentration. These investigations [22–24] have shown that cationic surfactants induce a discrete collapse from the DNA coil to a more compact globular form, and, moreover, that DNA globules and coils coexist. More interestingly, at surfactant concentration above the critical aggregation concentration, DNA-surfactant association, favored by both electrostatic interactions and hydrophobic self-association, applies preferentially to a DNA subpopulation, yielding a population of DNA-surfactant complexes in equilibrium with DNA molecules (coexistence of DNA globules and DNA coils).

At liposome concentration equal to or larger than $C_L=0.06$ mg/ml, but below the isoelectric condition, all the DNA chains present in the sample assume a more compact globule conformation, whose average size increases with the increase of the DOTAP liposome concentration. Consequently, the population associated with the DNA coil conformation disappears. In this range, the liposome concentration controls the degree of compaction, increasing the number of liposomes complexed per chain and inducing an overall shrinking of the chain. At the end of the process, above the isoelectric condition, each compact globule rearranges into a tight assembly of DNA-coated liposomes (charge inversion).

The existence of a bimodal distribution of DNA structures is also supported by electrophoretic mobility measurements that provide evidence of the presence of two different aggregates, one of them with a mobility equal to that of the unperturbed DNA chain (DNA coil) and the second one with a larger mobility, corresponding to DNA globules. It is worth noting the complete correspondence between the dynamic light scattering and the electrophoretic mobility results, where to the bimodal distribution in the correlation function corresponds a two-peak distribution in the electrophoretic mobility spectrum. Moreover, when the correlation function becomes mono-modal, corresponding to the unique presence of DNA globules, in the electrophoretic mobility spectrum, the component associated with the DNA coils disappears and only the component associated with the DNA globules remains.

Further insights into the DNA-cationic liposome interaction could result from the radio-wave dielectric behavior of these systems. Here, interactions are mainly of electrostatic nature, where the counterion distribution in the vicinity of both the DNA chain and the liposomal vesicle exerts an important role. Dielectric techniques probe the overall electrical characteristics of the system, and, in particular, when we consider the spectrum in the radio-wave frequency range, the observed relaxations are to be ascribed to the polarization arising from the nonuniform distribution of counterions around charged objects (negatively charged DNA and positively charged DOTAP liposomes) induced by the external electric field.

The dielectric properties of DNA aqueous solutions are generally attributed to an electric polarization mechanism of the counterion atmosphere along the polyion chain. This mechanism has been formerly proposed by Oosawa [25] and, later, by Mandel and co-workers [26–28].

Within this model, the DNA chain is represented by a sequence of rigid subunits of identical length b, and, in solution, because of its partially flexible structure, assumes a conformation characterized by a radius of gyration R_g. Counterion fluctuation occurs on two typical scale lengths, the overall length $L=(12R_g^2+b^2)^{1/2}$, causing a low-frequency relaxation process, and the subunit length b, causing a high-frequency relaxation process. The overall dielectric spectrum will be, therefore, composed of the superposition of two different relaxation processes, the one at low frequency and the one at high frequency, proportional to the average square end-to-end distance $\langle L^2\rangle$ of the whole polyion and to the square of the length b of the subunit, respectively. Here, we are focusing exclusively on the high-frequency relaxation mechanism.

As far as this mechanism is concerned, the dielectric increment $\Delta\epsilon$ and the relaxation frequency ν_0 are given by

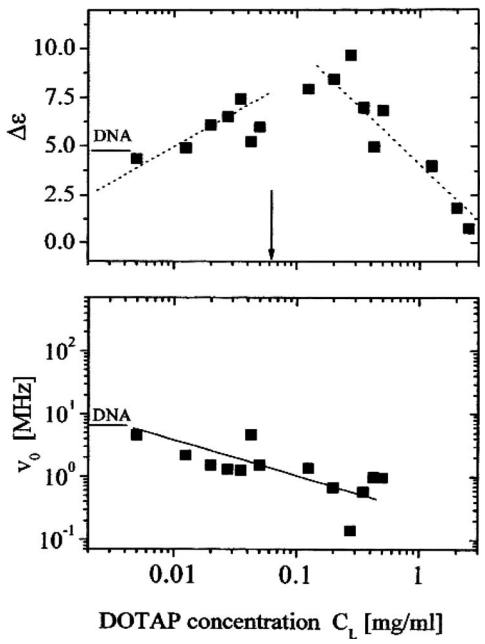

FIG. 3. Upper panel: Dielectric increment $\Delta\epsilon$ of DNA solution in the presence of DOTAP liposomes at different concentrations C_L. The uncertainties are within 10%. Dotted lines, drawn for visual purposes only, mark the liposome concentration (indicated by the arrow) at which the unperturbed DNA chains disappear, and only compacted globules are present. The dielectric increment of the pure DNA solution (at the concentration of C=0.75 mg/ml) is also indicated. Bottom panel: Relaxation frequency ν_0 of DNA solution in the presence of DOTAP liposomes at different concentrations C_L. The estimated uncertainties are within 20–30 %. The relaxation frequency of the pure DNA solution (at the concentration of C =0.75 mg/ml) is also indicated. In the DOTAP-DNA interaction, the DNA concentration is maintained constant at the value C =0.75 mg/ml.

$$\Delta\epsilon = \frac{(ze)^2 CfNb^2}{36\epsilon_0 k_B T}, \tag{3}$$

$$\nu_0 = \frac{\pi u k_B T}{2b^2}, \tag{4}$$

where C is the concentration of the polyion per unit volume, N the total number of charged sites per polyion chain, f the average fraction of associated counterions, ze their charge, ϵ_0 the dielectric constant of free space, u the mobility of counterions along the subunit b, and k_BT the thermal energy.

The dielectric properties of the DOTAP liposome-DNA complexes are shown in Fig. 3, where the dielectric increment $\Delta\epsilon$ and the relaxation frequency ν_0 are reported as functions of the DOTAP liposome concentration C_L. As can be seen, the dielectric increment $\Delta\epsilon$ inverts its trend at a DOTAP concentration C_L (approximately C_L=0.06 mg/ml), corresponding to the one at which both dynamic light scattering and electrophoretic measurements evidence the extinction of the free DNA component. From this point on, $\Delta\epsilon$ decreases with increasing concentration C_L, and it approaches zero close to the isoelectric condition. The relaxation frequency ν_0, within the associated relatively large uncertainties, decreases with increase of the concentration C_L. When the dielectric increments are small, of the order of one or a few dielectric units, the deconvolution of the dielectric spectra is rather difficult, and the results may be largely controversial. For this reason, we have omitted values of the relaxation frequencies close to the isoelectric condition.

The analysis of the dielectric parameters $\Delta\epsilon$ and ν_0 is rather intricate, because of the simultaneous presence, at low DOTAP liposome concentration, of DNA chains in two different conformations (coils and globules). However, the situation becomes plainer for DOTAP concentration higher than C_L=0.06 mg/ml, where the free DNA chain component disappears, and only the more compacted DNA component is present. In this context, the above-stated dielectric model applies and the two characteristic parameters, the subunit length b and the fraction f of associated counterions, can be evaluated. Assuming for the ion mobility u the value for the Na^+ ion in the high-dilution limit ($u=3.1\times10^{11}$ m/s N), the length b of the subunits varies from about 50 to about 150 nm as the DOTAP concentration increases from 0.06 to 1.2 mg/ml. In the same concentration range, the factor f decreases from 20% to 2%. This behavior shows a general agreement with the findings by Bonincontro *et al.* [29], who investigated, by means of dielectric methods, interactions of the cationic surfactant CTAB with DNA, on the basis of the Mandel model [Eqs. (3) and (4)]. These authors found that the fraction f of bound counterions, proportional to $\Delta\epsilon/b^2$, decreases approximately linearly with increasing molar ratio [CTAB]/[DNA] between surfactant monomers and DNA phosphate groups, suggesting that each CTAB monomer binds to a DNA phosphate group, provoking the release of a Na^+ ion. Moreover, the highly cooperative nature of the binding seems to be driven by hydrophobic association of the surfactant molecule tails. In the present case, for concentrations higher than C_L=0.06 mg/ml, at which the free DNA vanishes, the fraction f of associated counterions, normalized to the initial value f_0, decreases with increasing concentration C_L (or, conversely, with the charge ratio ξ =[DOTAP]/[DNA]) with a slope $m=-(2.2\pm0.4)$, not too different from the value $m=-(1.9\pm0.3)$ found for CTAB-DNA interactions [29]. Although at a qualitative level, this result suggests that interactions involve single lipid monomers with the release of counterions in the bulk solution.

B. DNA addition to a DOTAP liposome suspension

A different experimental procedure to induce DNA-DOTAP liposome interactions results in a rather different phenomenology that follows what happens in charged particle colloidal suspensions when aggregation is provoked by adding an oppositely charged polyion. In the past, we have investigated in detail this complex phenomenology, giving rise to two peculiar correlated effects known as reentrant condensation and charge inversion (or *overcharging*). We have extensively described these effects in a particular system, composed of charged liposomes built up by cationic DOTAP lipids and by a linear, rather flexible polyanion, poly(acrylate) sodium salt, which acts as an electrostatic glue [30–33].

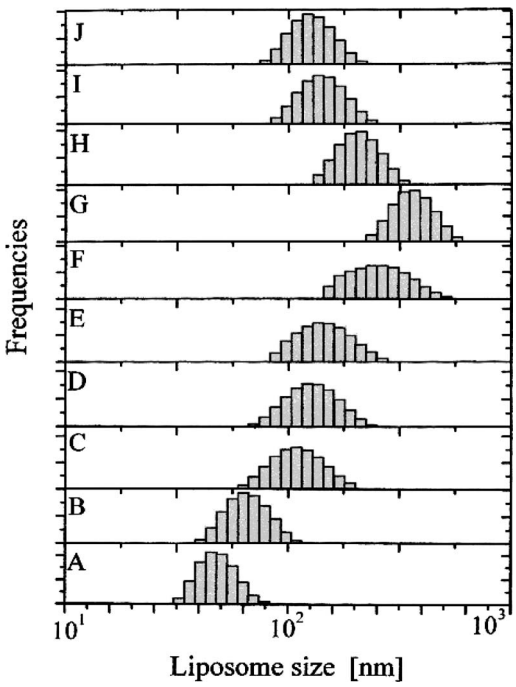

FIG. 4. Distribution of the hydrodynamic diameter of complexes formed between DOTAP liposomes and DNA obtained from the intensity-weighted NNLS algorithm analysis at the temperature of 25 °C, at different DNA concentrations C. (A) DOTAP liposome suspension, C_L=0.75 mg/ml; (B) C=0.005 mg/ml; (C) C =0.0125 mg/ml; (D) C=0.0275 mg/ml; (E C=0.042 mg/ml; (F) C=0.125 mg/ml; (G) C=0.275 mg/ml; (H) C=0.3 mg/ml; (I) C =1.0 mg/ml; (J) C=1.25 mg/ml.

In the present case, the DOTAP concentration was maintained fixed to the value of C_L=0.75 mg/ml (corresponding to a vesicle concentration of 8×10^{12} liposome/ml) and the concentration of DNA was varied from C=0.005 mg/ml (0.015 mM/l) to 2.5 mg/ml (7.6 mM/l).

The two typical effects, reentrant condensation and charge inversion, are shown in Figs. 4 and 5, where the size distribution of the liposome aggregates, derived from dynamic light scattering, and the sign of the overall charge, associated with the ζ potential, are shown as a function of the DNA concentration. Here, we present the ζ potential of the aggregates, instead of their electrophoretic mobility u, as we did in Sec. III A, in order to comply with the more common parameter in colloidal systems. However, these two quantities describe essentially the same electrokinetic parameter, by virtue of the Smolukowski relationship.

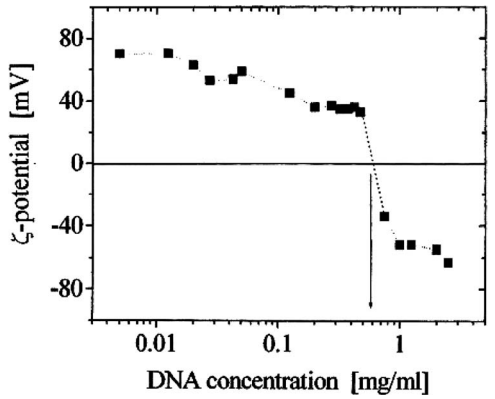

FIG. 5. ζ potential of DNA-induced DOTAP liposome complexes as a function of the DNA concentration. The arrow marks the DNA concentration corresponding to the inversion of sign of the ζ potential (isoelectric condition).

As can be seen, at low DNA content, the hydrodynamic radius of the liposomes is about 40 nm. Then, with increase of the DNA content, complexation begins with the formation of relatively small isolated DNA-coated liposomal particles, and no larger structures exist. In these conditions, the deconvolution of the scattered light intensity correlation function reveals that a single monomodal size distribution is present. Its average size corresponds to that of the liposomal particles. In other words, single DNA chains are not present, and the whole DNA interacts with the liposomes. The size of the complexes gradually increases until a maximum of the order of 550–600 nm is reached. Further increase of the DNA content determines the formation of decreasing-size complexes, until the size of the original liposomes is approximately reached again (reentrant condensation), indicating that, in these conditions, the resulting structures are stable against any further aggregation. Contrary to what happens when interactions occur in DNA excess (Sec. III A), only one population is present, i.e., DNA chain complexed within the liposomal structures (DNA-coated liposome particle clusters).

Corresponding to this complex average size evolution, aggregates undergo the charge inversion effect, documented by the ζ-potential values (Fig. 5) whose sign changes at the isoelectric condition, differentiating positive charge aggregates before the isoelectric condition from negative charge aggregates above the isoelectric condition.

The formation of a cluster phase composed of almost intact liposomes stuck together by oppositely charged DNA chains is further evidenced by the electrical (dielectric and conductivity) properties of the system.

As far as the electrical conductivity σ of DNA-DOTAP liposome complexes is concerned, its behavior as a function of the DNA concentration C is shown in Fig. 6(a). As can be seen, the increase of the electrical conductivity changes its slope markedly, in correspondence with the isoelectric point, where the overall charge of the liposome is almost compensated by the adsorbed DNA chains.

The formation of relatively large DNA-glued liposome clusters is favored by the entropy gain as a consequence of the release of counterions that are initially condensed on the DNA as well as on the liposomal particles. This counterion increase has been explained in terms of *lateral correlation* between adsorbed polyion chains on a charged surface [34–36]. On purely cationic lipid bilayers, DNA forms a highly ordered two-dimensional smectic phase with a regular spacing between adjacent DNA strands [37–39]. The liposome surface appears decorated by a more or less ordered "patchworklike" pattern, with excess negative charge (polyion-rich) domains and excess positive charged (polyion-free) domains, whose interactions impart the short-range attractive particle-particle potential ("charge patch" attraction). Close enough to the isoelectric point, the relatively small

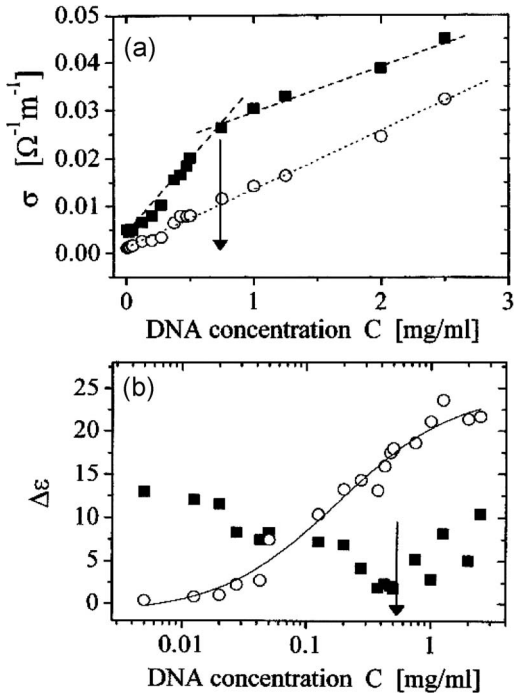

FIG. 6. (a) Electrical conductivity of DNA-liposome aggregates (■) and DNA solution (○) as a function of the DNA concentration C. The arrow marks the isoelectric condition, where the aggregates reach their maximum size and a different counterion release effect is evidenced. The dotted lines are calculated according to Eqs. (7) and (8). They intersect at the concentration corresponding to the isoelectric condition. (b) Dielectric increment $\Delta\epsilon$ of DNA-liposome aggregates (■) and DNA solution (○) as a function of the DNA concentration. The arrow marks the isoelectric condition, where the aggregates reach their maximum size and the dielectric increment $\Delta\epsilon$ approaches zero.

electrostatic repulsion balances this charge path attraction, and liposomes aggregate, forming large equilibrium clusters.

An analysis of the conductivity behavior of the system, similar to the one we have carried out previously [36] in the case of DOTAP liposome clusters stuck together by a synthetic polyanion, poly(acrylate) sodium salt, furnishes quantitative support for this view.

The electrical conductivity σ of the liposome aggregate suspension, during the whole DNA-induced complexation, can be easily calculated by assuming additivity and considering the contribution of the counterions alone. In the absence of DNA chain adsorption onto the liposome surface, the electrical conductivity resulting from ions (Na^+) derived from the partial ionization of the DNA chain and from the ions (Cl^-) derived from the partial ionization of the liposome particles, can be written as

$$\sigma = n(1-f)N_p\lambda_{Na^+} + (1/2)(1-g)N_L\lambda_{Cl^-}, \tag{5}$$

where the fractions $(1-f)$ and $(1-g)$ take into account the charge renormalization on both the DNA chain and the liposome, respectively, N_p and N_L are their concentrations (in mol/cm^3), λ_{Na^+} and λ_{Cl^-} are the equivalent conductances (expressed as Ω^{-1} cm^2 mol^{-1}) of Na^+ and Cl^- ions, respectively, and n is the number of monomers in each polyion chain.

In the DNA chain adsorption process, part of the condensed charges is released in the bulk solution, contributing to an increase of the electrical conductivity. According to the theory of correlated adsorption proposed by Nguyen *et al.* [35,40], upon adsorption, all polyion chains release a number of ions given by $N_p n(1-f)(\eta^*/\eta_c - 1)$, where η^* and η_c are the effective charge density after and before the adsorption. Nguyen *et al.* [40] give the following expression for η^*/η_c:

$$\eta^*/\eta_c = \sqrt{\frac{\ln(r_s/a)}{\ln(A_0/2\pi a)}}, \tag{6}$$

where r_s is the screening length due to monovalent counterions in the bulk solution, $A_0 = \eta_c/\sigma_0$ the spacing between the adsorbed polyion on the liposome surface with a surface charge density σ_0, and a the radius of the polyion. Consequently, upon adsorption, the electrical conductivity becomes

$$\sigma = n(1-f)N_p(\eta^*/\eta_c)\lambda_{Na^+} + (1/2)(1-g)N_L\lambda_{Cl^-}. \tag{7}$$

The renormalization factors g and f can be obtained, as is usually done in the electrical conductivity theories of polyelectrolyte solutions [41], from measurements of single liposome suspensions and single DNA solutions.

Assuming for the equivalent conductance of the counterions their values at infinite dilution ($\lambda_{Na^+} \simeq 50.2\ \Omega^{-1}$ cm^2 equiv^{-1} and $\lambda_{Cl^-} \simeq 76.4\ \Omega^{-1}$ cm^2 equiv^{-1}), Eq. (7) furnishes the expected values during the whole adsorption process, up to the isoelectric condition, where polyions cease to adsorb in order to neutralize the liposome charge, and further adsorption contributes only to the charge inversion.

From the isoelectric condition on, the electrical conductivity is described by the relation

$$\sigma = \sigma_{IEC} + n(1-f)N_p\lambda_{Na^+} \tag{8}$$

where σ_{IEC} is the conductivity at the isoelectric condition. Equations (7) and (8) intersect at the isoelectric condition, with two different slopes.

As can be seen in Fig. 6(a), the agreement of Eqs. (7) and (8) with the experimental data is rather good, over all the DNA concentration investigated. These results clearly show that the release of counterions from the polyions, and, partially, from the liposome particle surface, is the key parameter in the organization of the resulting aggregates.

Let us now turn to the dielectric properties. The dielectric properties of the aggregates in the different stages of the aggregation process, from single-DNA-decorated liposome to DNA-decorated liposome clusters, can be easily understood in the framework of the standard electrokinetic model [42–45], for a suspension of spherical mesoscopic objects.

Within this model, the dielectric increment $\Delta\epsilon$ of the dielectric relaxation associated with the counterion polarization in the vicinity of each charged aggregate is given by

$$\Delta\epsilon = \frac{9}{16} f(\zeta)\Phi\epsilon_m(K_D R_H)^2, \tag{9}$$

where $K_D = \sqrt{\sigma_m/D\epsilon_m}$ is the inverse of the Debye screening length, ϵ_m and σ_m are the permittivity and the electrical con-

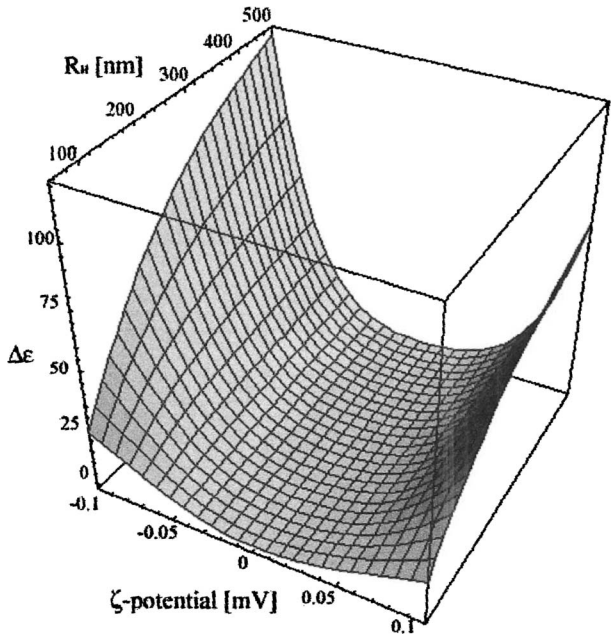

FIG. 7. Dependence of the dielectric increment $\Delta\epsilon$ as a function of the ζ potential and the hydrodynamic radius R_H of the aggregates calculated in the framework of the standard electrokinetic model. The values of the parameters are as follows: viscosity of the aqueous phase $\eta=1$ cP; permittivity of the aqueous phase $\epsilon_m=78.5$; electrical conductivity of the aqueous phase $\sigma_m=0.02\ \Omega^{-1}\ m^{-1}$; counterion diffusion coefficient $D=10^{-9}\ m^2/s$; fractional volume of the dispersed phase $\Phi=0.01$.

ductivity of the aqueous phase, respectively, R_H is the hydrodynamic radius of the vesicle, D is the diffusion coefficient of counterions, and $f(\zeta)$ is a function depending on the ζ potential of the liposome particle and on the environmental parameters that define the system. This function is defined in detail in Ref. [43].

A typical behavior of the dielectric increment $\Delta\epsilon$ calculated on the basis of Eq. (9) as a function of both the ζ potential and the average size R_H of the aggregates is shown in Fig. 7. The strength of the dielectric relaxation increases as the ζ potential deviates from zero on both sides and, at the same ζ potential, with the increase of the average size R_H. Equation (9) furnishes a quite good agreement with the experimental data.

Once the environmental parameters of the systems (the permittivity ϵ_m, the electrical conductivity σ_m, and the viscosity η of the aqueous phase) are known, the measurement of the ζ potential and of the hydrodynamic radius R_H of the liposome aggregates during the whole aggregation process induced by the DNA addition (for a detailed analysis of the ζ potential and R_H behavior, see Refs. [12,34]) allows us to calculate the expected values of $\Delta\epsilon$. We have compared these values with those experimentally observed in Fig. 8. Considering that there is no adjustable parameter, the agreement is quite good.

It must be noted, however, that the applicability of the above-stated model suffers from two serious forcings. The first is that DNA-coated liposome aggregates are more similar to soft than to hard particles with a well-defined double-

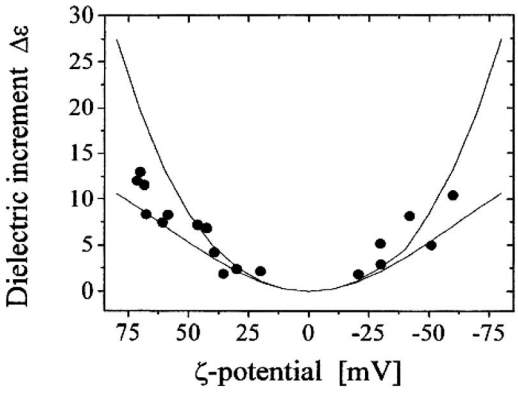

FIG. 8. Dependence of the dielectric increment $\Delta\epsilon$ of liposome clusters as a function of the ζ potential. The full curves are calculated according to Eq. (9), for two different values of the average size of the aggregates: upper curve, $R_H=200$ nm; lower curve, $R_H=55$ nm.

layer structure. The second one is that Eq. (9) is indiscriminately applied to the single-DNA-decorated liposome and to a cluster of DNA-decorated liposomes and, when aggregates become very large and heavily heterogeneous, the use of Eq. (9) may be questionable. In spite of these restraints, the main features of the dielectric behavior are well described within the classical electrokinetic model for mesoscopic particle colloidal suspensions.

C. Further comments on the mode of DNA-DOTAP aggregate formation

Even though a general consensus has not been reached yet, there are different experiments that show differences in the DNA-lipid aggregates, depending upon whether complexes are formed by the addition of DNA to lipids or, vice versa, by the addition of lipid to DNA. These aspects are considered in detail by Kennedy *et al.* [46], who attributed the different behaviors to a difference in symmetry of the two components, DNA and cationic liposomes. These authors pointed out that the reason for this difference resides in the fact that lipids are organized in bilayer vesicles, and their wall stress differs if they interact with a small or a large amount of DNA. At a molecular level, the different behavior is related to the stoichiometry of the two components, DNA and liposomes, when the vesicles collapse in the aggregates. When DNA is added to the liposome suspension, the stoichiometry (lipids initially in excess) favors aggregates formed by liposomes stuck together by the oppositely charged DNA chains, and the phenomenology is well accounted for by the reentrant condensation and the charge inversion effects. In the reverse condition, when DNA is initially in excess, the process of compaction is gradual and the apparent size of the DNA chain decreases with increase of the number of liposomes per chain. In the case of solid nanoparticles, transmission electron microscope images [47] have shown bead-on-a-string structures, in which each bead corresponds to a nanoparticle onto which part of the DNA chain has been adsorbed. In the case of liposomal particles, a rupture of the

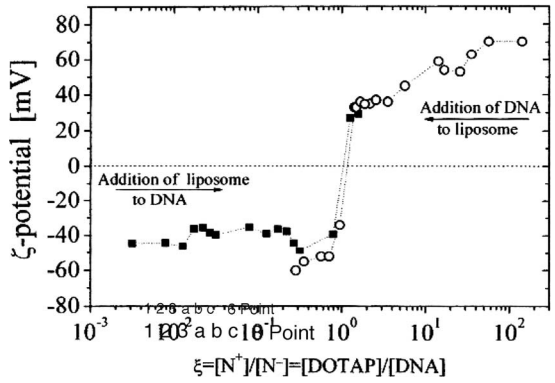

FIG. 9. Cumulative plot of the ζ potential as a function of the charge ratio $\xi=[N^+]/[N^-]$ between the positive charge of a lipid molecule and the negative charge of a DNA phosphate group. The data summarize the results obtained from the two different modes of formation of the aggregates, depending upon the order of addition, i.e., addition of lipid to DNA or addition of DNA to lipid. Aggregates evolve from structure with an overall negative charge (in DNA excess condition) to structures with an overall positive charge (in liposome excess condition).

lipid vesicle is expected, and the compaction phenomenology recalls that induced by cationic surfactants.

However, in the present case, owing to the large interval of DNA and/or DOTAP concentrations investigated, we are in the condition of presenting a unified description of the overall aggregation process, when the data, average size as determined from dynamic light scattering, and ζ potential, as determined by electrophoretic mobility measurements, are plotted as a function of the ratio $\xi=[N^+]/[N^-]=[\text{DOTAP}]/[\text{DNA}]$ between the positive charge of a lipid molecule and the negative charge of a DNA phosphate group. These plots (Figs. 9 and 10) clearly demonstrate the complete evolution of the aggregation and clearly evidence that there is a continuous transition from the initial DNA

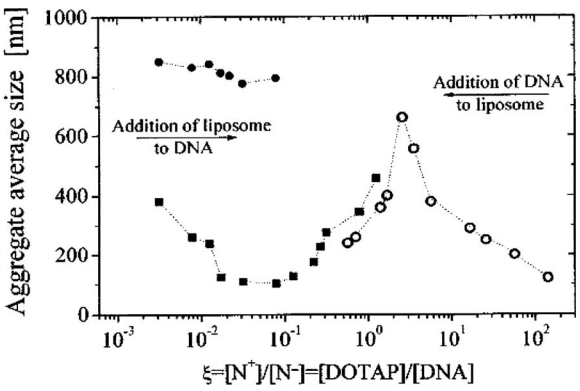

FIG. 10. Cumulative plot of the average size $2R_H$ of the aggregates as a function of the charge ratio $\xi=[N^+]/[N^-]$ between the positive charge of a lipid molecule and the negative charge of a DNA phosphate group. The data summarize the results obtained from the two different modes of formation of the aggregates, depending upon the order of addition, i.e., addition of lipid to DNA or addition of DNA to lipid.

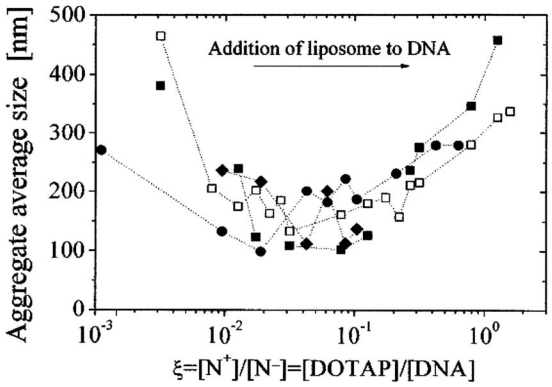

FIG. 11. Average size $2R_H$ of the aggregates as a function of the charge ratio $\xi=[N^+]/[N^-]$ between the positive charge of a lipid molecule and the negative charge of a DNA phosphate group. The data summarize the results obtained by means of different algorithms employed in the Laplace inversion of the intensity-intensity autocorrelation function, (■) non-negative least-squares NNLS algorithm; (□) CONTIN algorithm. Different molecular weight DNA does not change appreciably the whole behavior of the complexation: (●) double-stranded DNA after sonication, about 500 base pairs (bp); (◆) double-stranded DNA, molecular weight between 5 and 10 kbp molecular weight.

compaction, with the coexistence of coils and globules, to the formation of larger and larger liposome aggregates (close to the isoelectric condition), and finally to small liposomal aggregates of inverted charge.

Although the average size and ζ-potential measurements are somewhat noncongruent, close to the isoelectric condition ($\xi \simeq 1$), they are similar enough, considering that all the measurements were made with different preparations and at different times. It is worth noting that DNA compaction and coil-globule coexistence end when the DNA reaches its minimum size, and, from this point on, the process proceeds with the formation of DNA-induced liposome aggregates.

Finally, we have investigated more deeply the formation of the aggregates during the addition of lipid to DNA. We employed double-stranded DNA of two different chain lengths, $(5-10)\times 10^3$ and 500 bp, respectively. The DNA concentration was maintained constant to the value of $C_{\text{DNA}}=1.1$ mg/ml and the concentration of DOTAP lipid was varied from 0.02 to 1.6 mg/ml. For both the two samples investigated, we obtain rather similar results (Fig. 11), and, in particular, the presence of the shallow minimum in the average size of the DNA chain, indicating the DNA compaction prior to the beginning of the reentrant condensation effect.

A final, technical, comment. Since the Laplace inversion of the intensity-intensity autocorrelation function is an ill-conditioned problem, in some cases, we do not know whether the size distribution function obtained by the NNLS algorithm [17] is reliable, or if is an artifact due to the algorithm itself. We then employed a different algorithm, CONTIN [16], a smoothing technique combined with a regularization method. The two algorithms give values in rather good agreement. A comparison between the two set of results is shown in Fig. 11. This agreement gives further support to the analysis above.

IV. CONCLUSIONS

DNA-cationic liposome interaction results in the formation of two differently organized complexes, according to the way the interaction takes place. In cationic liposome excess, DNA addition favors the formation of liposome clusters whose size and overall charge obey the reentrant condensation and the charge inversion effects. In other words, liposomes, which maintain their integrity, aggregate, originating a cluster phase with new and peculiar characteristics. These aspects have been extensively investigated in a series of previous works [30–33] concerning aggregation of DOTAP liposomes induced by a synthetic polyanion, poly(acrylate) sodium salt. The strong analogy evidenced between these two systems suggests that the above-stated phenomenology is largely independent of the chemical nature of the polyions, whose correlated adsorption at the liposome surface imparts the short-range attractive interactions which control the aggregation. We have schematized the role of the polyions as that of an electrostatic glue, able to stick together different liposomes.

In DNA excess, the phenomenology is rather different, the basic structures continuing to be the DNA chains which coexist in two different conformations, coils and globules. The overall charge of these two structures continue to be negative up to the isoelectric condition, resembling the charge of the DNA chain. The system does not experience either charge inversion or reentrant condensation, as happens in the liposome cluster phase for DNA-liposome systems, in liposome-excess condition. In this case, during interactions between DNA and cationic liposomes, DNA compaction is accompanied by liposome rupture with the formation of DNA-lipid complexes.

These two different pictures can be reconciled when the experimental data are represented as a function of the charge ratio ξ, giving support to the possibility of describing apparently different phenomena in a unified way.

Recently, Zinchenko *et al.* [47], on the basis of microscopic observation and molecular dynamics simulations, have individuated, in single-chain DNA-solid nanoparticle complexation, three distinct cases that they call adsorption, wrapping, and collection. All these modes are favored by the semiflexible nature of the DNA chain and are governed by the ratio between the persistence length of the DNA chain and the size of the nanoparticle. The first one (adsorption) occurs preferentially in large particles, whose surface becomes the site of a two-dimensional adsorption. The second one (wrapping) becomes relevant when the particle size is smaller than the persistence length, and the adsorption is realized by one or a few turns of the DNA chain around the particle. Finally, the third one (collection) is realized when particles are much smaller that the chain and wrapping becomes a high-energy cost process.

In the present case, we observe the above-stated basic phenomenology where the two mechanisms (adsorption and wrapping), when considered in an ensemble in an ensemble of DNA chains, rather than in a single chain, lead to the formation of polyion-coated particle aggregates (interactions in DOTAP-liposome-excess condition, Sec. III B). In the DNA-chain-excess condition, especially for long chains, the collection mode dominates and the single nanoparticles adsorb on the DNA chain. However, when particles are realized by lipidic liposomes, the rupture of these structures and their reorganization with the DNA chains yields the compaction of DNA and the simultaneous presence of coils and globules (interactions in DNA-excess condition, Sec. III A).

ACKNOWLEDGMENT

This work is supported in part by INFM-CNR, Research Center SOFT, Unità di Romal an Unità di Perugia.

[1] A. Zinchenko and N. Chen, J. Phys.: Condens. Matter **18**, R453 (2006).
[2] D. Lasic, Trends Biotechnol. **16**, 307 (1998).
[3] T. Allen and P. Cullis, Science **303**, 1818 (2004).
[4] S. Mel'nikov, V. Sergeryeu, and K. Yoshikawa, J. Am. Chem. Soc. **117**, 2401 (1995).
[5] K. Wagner, D. Harries, S. May, V. Kahl, J. Rädler, and A. Ben-Shaul, Langmuir **16**, 303 (2000).
[6] S. Mel'nikov, V. Sergeryeu, K. Yoshikawa, H. Takahashi, and I. Hatta, J. Chem. Phys. **107**, 6917 (1997).
[7] S. Marchetti, G. Onori, and C. Cametti, J. Phys. Chem. B **110**, 24761 (2006).
[8] M. Cardenas, K. Schillen, T. Nylander, J. Jansoson, and B. Lindman, Phys. Chem. Chem. Phys. **6**, 1603 (2004).
[9] V. Bloomfield, Curr. Opin. Struct. Biol. **6**, 334 (1996).
[10] E. Raspaud, D. Durand, and F. Livolant, Biophys. J. **88**, 392 (2005).
[11] A. Stradner, H. Sedgwick, F. Cardinaux, W. Poon, S. Egelhaaf, and P. Schurtenberger, Nature (London) **432**, 492 (2004).
[12] F. Bordi, C. Cametti, M. Diociaiuti, and S. Sennato, Phys. Rev. E **71**, 050401 (2005).
[13] A. Yethiraj and A. van Blaaderen, Nature (London) **421**, 513 (2003).
[14] P. Lu, J. Conrad, H. Wyss, A. Schfield, and D. Weitz, Phys. Rev. Lett. **96**, 028306 (2006).
[15] F. Sciortino, S. Mossa, E. Zaccarelli, and P. Tartaglia, Phys. Rev. Lett. **93**, 055701 (2004).
[16] S. W. Provencher, Comput. Phys. Commun. **27**, 229 (1982).
[17] C. L. Lawson and R. J. Hanson, *Solving Least Squares Problems* (Prentice-Hall, Englewood Cliffs, NJ, 1974).
[18] S. Takashima, A. Casaleggio, F. Giuliano, M. Morando, P. Arrigo, and S. Ridella, Biophys. J. **49**, 1003 (1986).
[19] F. Bordi, C. Cametti, and G. Paradossi, Biopolymers **40**, 485 (1996).
[20] F. Bordi, C. Cametti, and T. Gili, Bioelectrochemistry **54**, 53 (2001).
[21] R. Dias, J. Innerlohinger, O. Glatter, M. Miguel, and B. Lindman, J. Phys. Chem. B **109**, 10458 (2005).
[22] R. S. Dias, A. C. Pais, M. G. Miguel, and B. Lindman, Colloids Surf., A **250**, 115 (2004).

[23] R. Dias, S. Mel'nikov, B. Lindman, and M. Miguel, Langmuir **16**, 9577 (2000).
[24] S. Mel'nikov, V. G. Sergeyev, and K. Yoshikava, in *Recent Research Development in Chemical Sciences*, edited by S. G. Pandalai (World Scientific, Singapore, 1997), p. 69.
[25] F. Oosawa, *Polyelectrolytes* (Marcel Dekker, New York, 1971).
[26] M. Mandel, Ann. N.Y. Acad. Sci. **303**, 74 (1977).
[27] T. Vreugdenhil, F. van der Touw, and M. Mandel, Biophys. Chem. **10**, 67 (1979).
[28] F. van der Touw and M. Mandel, Biophys. Chem. **2**, 218 (1971).
[29] A. Bonincontro, S. Marchetti, G. Onori, and A. Rosati, Chem. Phys. **312**, 55 (2005).
[30] F. Bordi, C. Cametti, C. Marianecci, and S. Sennato, J. Phys.: Condens. Matter **17**, 1 (2005).
[31] S. Sennato, F. Bordi, C. Cametti, M. Diociaiuti, and P. Malaspina, Biochim. Biophys. Acta **1714**, 11 (2005).
[32] F. Bordi, C. Cametti, and S. Sennato, Chem. Phys. Lett. **409**, 134 (2005).
[33] F. Bordi, C. Cametti, S. Sennato, and D. Viscomi, J. Chem. Phys. **126**, 024902 (2007).
[34] S. Sennato, F. Bordi, and C. Cametti, Europhys. Lett. **68**, 296 (2004).
[35] T. Nguyen and B. Shklovskii, J. Chem. Phys. **114**, 5905 (2001).
[36] F. Bordi, C. Cametti, and S. Sennato, Phys. Rev. E **74**, 030402(R) (2006).
[37] H. Clausen-Schaumann and H. Gaub, Langmuir **15**, 8246 (1999).
[38] J. Rädler, I. Koltover, T. Salditt, and C. Safinya, Science **275**, 810 (1997).
[39] Y. Fang and J. Yang, J. Phys. Chem. **101**, 3453 (1997).
[40] T. Nguyen and B. Shklovskii, Rev. Mod. Phys. **74**, 329 (2002).
[41] F. Bordi, R. H. Colby, C. Cametti, L. De Lorenzo, and T. Gili, J. Phys. Chem. B **106**, 6887 (2002).
[42] S. Dukhin and V. Shilov, in *Interfacial Electrokinetics and Electrophoresis*, edited by A. Delgago (Dekker, New York, 2001).
[43] C. Grosse, *Encyclopedia of Surface and Colloid Science* (Elsevier, Amsterdam, 2002).
[44] C. Grosse, *Interfacial Electrokinetics and Electrophoresis*, edited by A. V. Delgado (Marcel Dekker, New York, 2001).
[45] M. Tirado, C. Grosse, W. Schrader, and U. Kaatze, J. Non-Cryst. Solids **305**, 373 (2002).
[46] M. T. Kennedy, E. V. Pozharski, A. Rakhmanova, and R. C. MacDonald, Biophys. J. **78**, 1620 (2000).
[47] A. Zinchenko, T. Sakaue, S. Araki, K. Yoshikawa, and D. Baigl, J. Phys. Chem. B **111**, 3019 (2007).